Improved Flight Flutter Testing Excitation Techniques

Final Report

EOARD Contract F61775-98-WE012

Dynamics and Control Research Group, School of Engineering, University of Manchester, UK.

Reference: DCRG /98/ EOARD/2

Date of issue: 28th September 1998

Written by: Dr. M.J. Desforges & Dr J.E. Cooper

Authorised by: Dr J.E. Cooper

Distribution: EOARD   J. J. Sellars
                   AFOSR/NA   B. Saunders
                   USAF   B. Shirley
                   NASA Dryden   R. Lind
                   Univ of Manchester M.J. Desforges
                                      J.E. Cooper
                                      J.R. Wright

19981216 031

AQF99-03-0340

REPORT DOCUMENTATION PAGE

Form Approved OMB No. 0704-0188

1. AGENCY USE ONLY (Leave blank)	2. REPORT DATE	3. REPORT TYPE AND DATES COVERED
	28 September 1998	Final Report

4. TITLE AND SUBTITLE	5. FUNDING NUMBERS
Improved Flight Flutter Testing Excitation Techniques	F61775-98-WE012

6. AUTHOR(S)

Dr. Jonathan Cooper

7. PERFORMING ORGANIZATION NAME(S) AND ADDRESS(ES)	8. PERFORMING ORGANIZATION REPORT NUMBER
School of Engineering , University of Manchester Oxford Road Manchester M13 9PL United Kingdom	N/A

9. SPONSORING/MONITORING AGENCY NAME(S) AND ADDRESS(ES)	10. SPONSORING/MONITORING AGENCY REPORT NUMBER
EOARD PSC 802 BOX 14 FPO 09499-0200	SPC 98-4026

11. SUPPLEMENTARY NOTES

12a. DISTRIBUTION/AVAILABILITY STATEMENT	12b. DISTRIBUTION CODE
Approved for public release; distribution is unlimited.	A

13. ABSTRACT (Maximum 200 words)

This report results from a contract tasking School of Engineering , University of Manchester as follows: The contractor will investigate improvements in excitations signals used in aircraft flutter flight test data collection. Complete description of the research program is contained in the proposal Statement of Work.

14. SUBJECT TERMS

EOARD, Aircraft Structures, Aerodynamics, Fluid Dynamics

15. NUMBER OF PAGES

45

16. PRICE CODE

N/A

17. SECURITY CLASSIFICATION OF REPORT	18. SECURITY CLASSIFICATION OF THIS PAGE	19. SECURITY CLASSIFICATION OF ABSTRACT	20. LIMITATION OF ABSTRACT
UNCLASSIFIED	UNCLASSIFIED	UNCLASSIFIED	UL

Summary

This report describes the work done during the period 1st April 1998 - 30th September 1998 for the EOARD contract F61775-98-WE012 on Improved Flight Flutter Testing Excitation Techniques. Strategies. A number of improved swept sine ('Chirp') and random excitation signals are developed and demonstrated to be superior to conventional linear sweeps and minimum crest factor random signals.

Table of Contents

1. Introduction

The vibration behaviour of an aircraft in flight is governed by the science of aeroelasticity [1], i.e. the interaction of the aerodynamic, inertial and elastic forces. There are a number of undesirable aeroelastic phenomena, and the most dangerous of these is flutter, which manifests itself as a violent unstable oscillation that often results in structural failure. Flutter has been the cause of numerous fatal accidents since it was first observed on a Handley Page 0/400 biplane in 1916 [2]. Current aircraft designs undergo sophisticated aeroelastic analysis, often coupled with wind tunnel tests, to ensure that flutter does not occur within the desired flight envelope. However, testing in flight is still required to validate the theoretical predictions and to ensure that the aircraft remains flutter free throughout the desired flight envelope. Such a test procedure is known as flight flutter testing.

Flight flutter testing is a critical step in the development of a prototype aircraft. The procedure to ensure a flutter free flight envelope is difficult, as discussed later, and flutter incidents still occur. Future aircraft designs that are lighter, more flexible and involve smart technologies are likely to place an even greater reliance on this part of the aircraft development procedure. Improvements in testing methodologies are still required in order to enhance the safety and efficiency of the process.

Essentially, the flight flutter test procedure consists of performing vibration tests in flight and tracking the estimated frequencies and damping values against speed or Mach number. There are three key stages:

1. at a constant flight condition the aircraft is excited in some manner (pilot induced inputs, control surface excitation via the flight control system, aerodynamic vanes, explosive devices, turbulence, etc.) and the response measured (usually with accelerometers) at various points on the structure.
2. the measured input and output data is curve-fitted, in either the time or frequency domains, using system identification algorithms in order to estimate the natural frequencies and damping ratios at that particular flight condition [3].
3. the decision is made to move to the next flight test point, based upon the estimated parameters, the trends of the damping ratios against speed or Mach number. Extrapolation methods are often used to predict the onset of flutter based upon the experimental results [3].

It is essential that the testing and curve-fitting is made as accurate as possible to enable a safe flutter clearance programme in as few flights as possible. It is the damping of the aircraft that is of greatest interest, however, this is the parameter that is most susceptible to experimental errors and corruption of the measured data. There are a number of difficulties that occur in flight flutter testing that lead to corruption of the measured data. The main problems are:

1. difficulties in providing adequate excitation - there are a limited number of ways of exciting the aircraft in flight

2. a limited number of response measurements - it is usual to use far fewer measurement channels (16-32) in flight compared to the corresponding ground vibration test (500 - 1500 channels).

3. noise, in particular due to turbulence - this becomes a greater problem at the edges of the flight envelope which is the most crucial part of the test procedure where good quality data is essential.

The combination of the above problems, along with the fact that an aircraft is a complex structure possessing multiple modes with close natural frequencies, means that the curve-fitting process is difficult. There can often be problems in identifying all of the required modes with a great deal of confidence and hence determining whether it is safe to proceed to the next test point. Many flights are therefore necessary for the flutter test clearance, particularly where multiple store cases need to be considered. The cost of such tests can be as much as $50k per flight test hour, and so it is highly desirable to develop improved testing methods that not only provide for safer testing, but also enable the number of flights to be reduced, thereby making a substantial saving of time and money. The USAF is interested in improving their flight flutter test capability for the certification of new weapon systems on the F-16 and F-15, as well as the future flutter clearance of the F-22.

A primary target area for improvement in flight flutter testing is the quality of the excitation applied to the aircraft. Excitation signals derived specifically for a given aircraft type or set of test conditions will improve the quality of both the measured input and response signals. The quality of response data may be simply evaluated in terms of the noise-to-signal ratio, NSR, defined as

$$NSR = \frac{RMS\ noise\ level}{RMS\ signal\ level} \tag{1}$$

where RMS denotes the root-mean-square amplitude of the time-domain signal. Clearly, maximising the NSR of the measured signals will improve the quality of the modal parameters ultimately calculated.

Previous work has been undertaken in the optimisation of random input signals through the reduction of the crest factor [4]. However, no consideration has been given to the implications of these signals on the rate and/or amplitude requirements of the actuators, or the effect on the crest factor and NSR of the response signal. Similarly, applications of sine sweeps for flight flutter testing have used conventional linear or logarithmic sweeps. In this work, the optimisation of both random and sine sweep signals will be considered for flight flutter testing, and in particular, improvements will be made to take account of rate, amplitude and other practical requirements relevant to flight flutter testing.

2. Optimal Sweep Excitation

2.1 Simple Sweep Signals

Frequency sweep or 'chirp' signals are the most popular form of continuous excitation used in vibration testing, and are particularly common in flight flutter testing. A chirp is a continuous signal whose frequency varies in some manner with time. As a result, the signal can contain power across a range of frequencies. A general chirp is defined by the expression

$$x(t) = a(t)\sin\left(\int_0^t 2\pi f(t)\, dt\right) \tag{2}$$

where both the frequency and the amplitude level may be varied with time. Although it is normal to increase frequency with time (sweep 'up'), it is equally possible to sweep 'down' in frequency. It should be noted that a sweep 'up' immediately followed by a sweep 'down' should not be used as an excitation signal in vibration testing. This type of input, used by some flight test practitioners, can result in a power spectrum with zero values at certain frequencies due to cancellation of parts of the sweep 'up' section by the sweep 'down' section with opposing phases [5]

2.1.1 Linear Chirp

The single section linear chirp is the simplest broadband excitation signal. The initial and final frequencies must be specified, along with the total duration of the signal and the amplitude level. The frequency of excitation is then varied linearly with time, such that

$$f = f_1 + \left(\frac{f_2 - f_1}{T}\right)t = f_1 + \alpha t \tag{3}$$

With reference to equations (2) and (3), the linear chirp is given by

$$x(t) = a\sin\left(2\pi\left\{f_1 t + \frac{\alpha t^2}{2}\right\}\right) \tag{4}$$

Although it is guaranteed that the chirp will start with a value of zero, there is no guarantee that the signal will end at zero. Therefore, the signal will, generally, be non-periodic and thus violate the requirements of the Fourier transform in subsequent analyses. In cases where only a single chirp is used as an input during vibration testing, a windowing function, such as a Hanning window, may be applied to ensure periodicity. Alternatively. a burst chirp signal may be employed where the chirp only occupies a fraction of the total time window, say 75%. In this case, the system response is

given time to decay to zero before the end of the time window and periodicity of both the input and response signals is ensured.

If it is required to use a continuous sequence made up of a number of chirps, neither windowing nor burst chirps are suitable. Instead, the chirp defined in equation (4) is extended at a constant sweep rate until it next crosses zero with a positive slope, and then is terminated. A sequence of such chirps will then follow a continuous variation, although the slope will be discontinuous at the joins. Clearly, the initial definition of the chirp has been compromised in that the final frequency has been changed to extend the signal. However, this is deemed a small price to pay for the avoidance of the leakage errors resulting from non-periodic signals. An additional point should be noted when the input signals are defined digitally, as opposed to in an analogue sense, for input into digital-to-analogue conversion (DAC) units. In this case, continuity of the sequence of signals can only be maintained if the final point of each chirp is negative, rather than non-zero, to match the zero first point of the next chirp section. The final point of the combined sequence, however, should be set to zero to ensure overall periodicity of the signal.

In this work, all chirp signals will be defined digitally and the above methods for ensuring continuity and periodicity of the final signal.

2.1.2 Logarithmic Chirp

The second class of chirp signals is the 'logarithmic chirp'. In this case, the sweep rate increases (or decreases) exponentially with time, giving a frequency variation of

$$f = f_1 \exp\left(\left\{\frac{1}{T}\ln\frac{f_2}{f_1}\right\}t\right) = f_1 \exp(\alpha t)$$ (5)

This time-dependent frequency variation results in a signal defined by

$$x(t) = a\sin\left(\frac{2\pi f_1}{\alpha}\left\{\exp(\alpha t) - 1\right\}\right)$$ (6)

Clearly, as for the linear chirp, there is no guarantee that the signal will be periodic within its time window. In cases where sequences of logarithmic chirps are to be used end-to-end, it will again be necessary to alter the length and/or final frequency of the chirp components to ensure continuity in the resulting signal.

The major perceived benefit of the logarithmic chirp as an excitation signal during vibration testing is that the same time is spent exciting the structure across the half power bandwidth of any mode having the same damping ratio. A linear chirp spends proportionally more time exciting modes with

7

higher natural frequencies and this may be sub-optimal. The difference between linear and logarithmic chirp inputs is particularly important is applications such as a flutter testing where the level of noise can be significant and optimal excitation of all modes is essential.

A simple linear chirp is illustrated in figures 1 and 2, with a simple logarithmic chirp illustrated in figures 3 and 4. In both cases, the chirp occupies 100% of the available time window, with no alterations made to ensure periodicity.
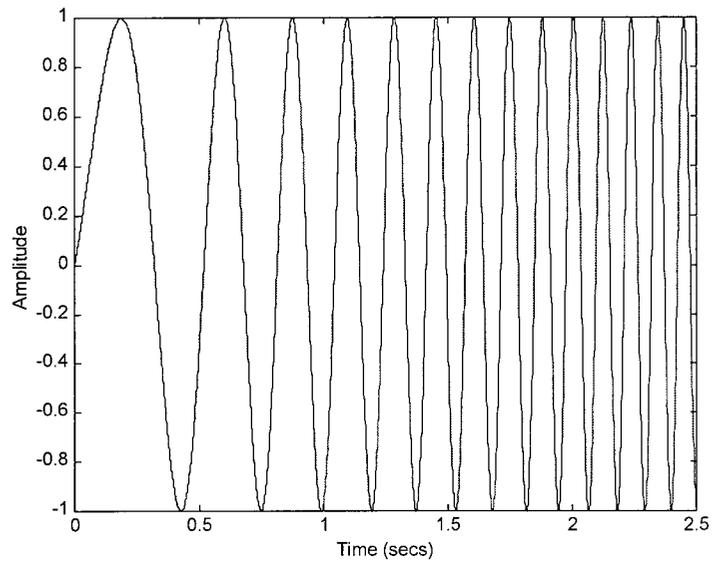
Figure 1 – Linear chirp signal
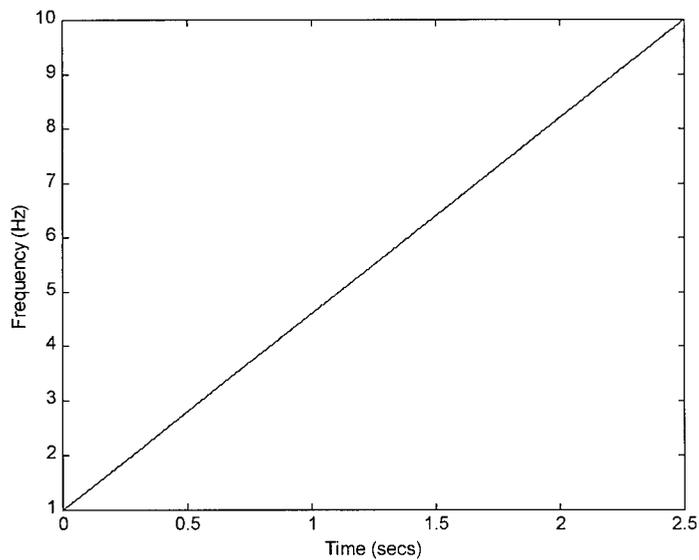
Figure 2 – Frequency variation of linear chirp signal

8
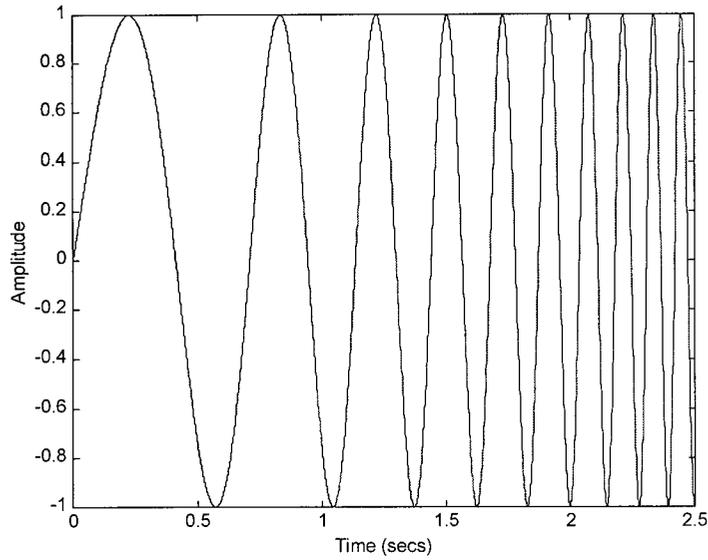
Figure 3 –Logarithmic chirp signal
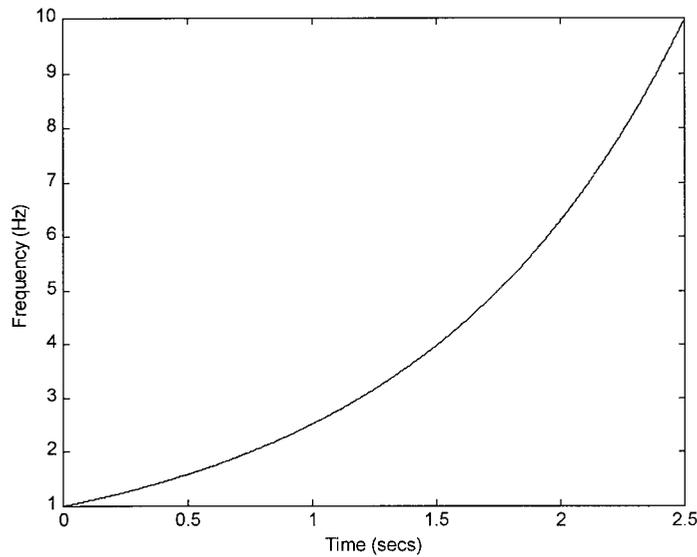
Figure 4 –Frequency variation of logarithmic chirp signal

2.2 Multi-section chirps

This type of signal is, as discussed above, a series of simple linear or logarithmic chirps placed end-to-end with continuity ensured at the joins. By specifying the frequency values at the breakpoints, certain frequency ranges may be concentrated upon and other swept through relatively quickly. In this way, simple optimisation of the input signal may be achieved.

Figure 5 shows a simple three section linear chirp, with the frequency variation shown in figure 6. Figure 7 shows the power spectrum of the input, demonstrating the additional power input in the central frequency band through the use of a slower frequency sweep rate.

9
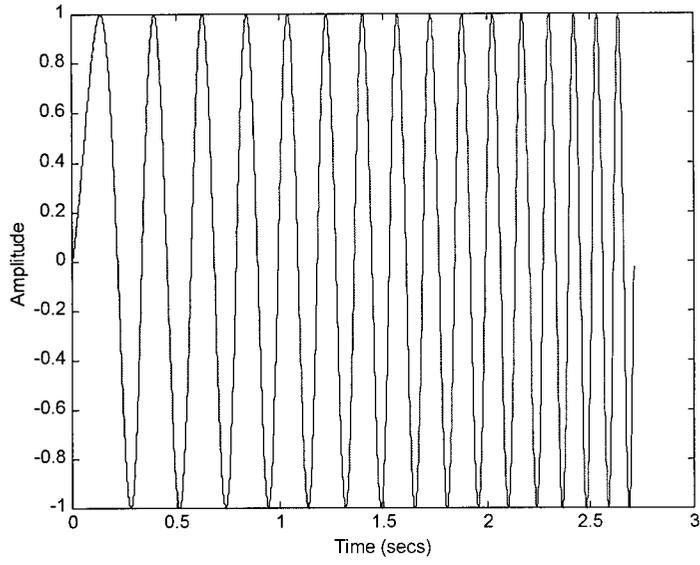
Figure 5 – Three section linear chirp signal
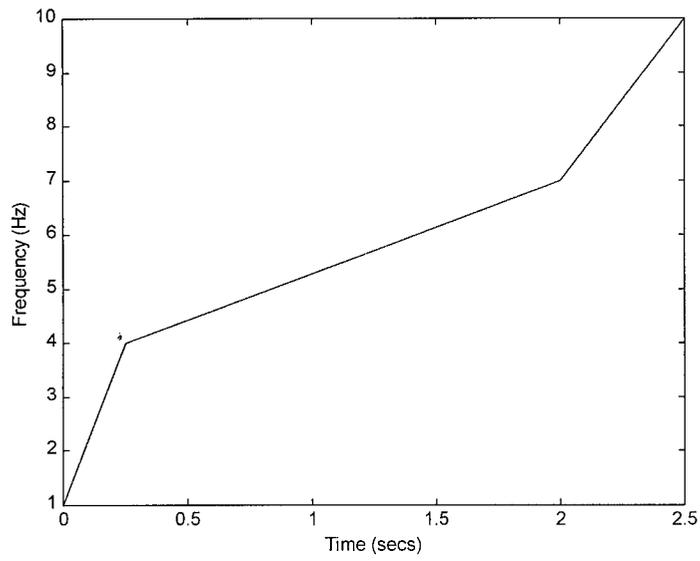
Figure 6 – Frequency variation of three section linear chirp signal
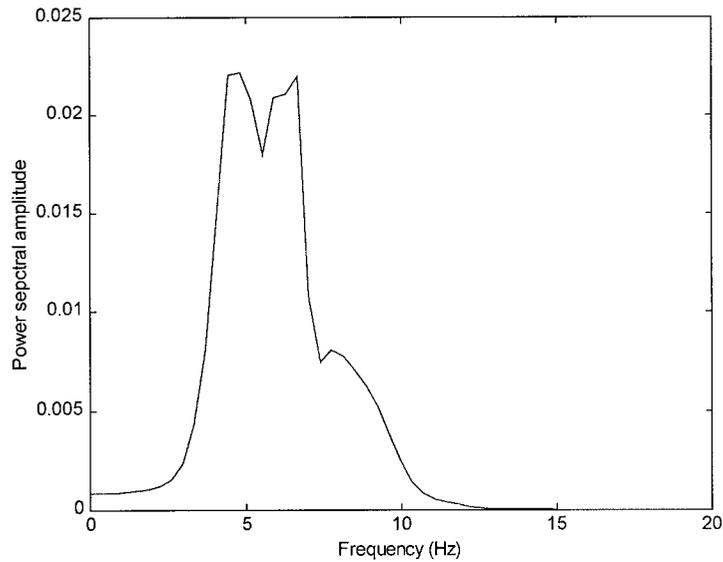
Figure 7 – Power spectrum of three section linear chirp signal

A further method of customising a chirp input signal is by varying the amplitude levels of the individual sections. Although continuity of the signal is assured between consecutive chirps of any positive amplitude levels, switches from large amplitude sections to small amplitude sections (or vice versa) will lead to significant discontinuities in the differential of the signal which may affect the response the system under test.

Figure 8 shows a three section linear chirp with variable amplitude levels and the frequency variation seen previously in figure 6. Continuity of the signal is seen even with the varying amplitude levels of the three sections. The power spectrum of the three section signal is shown in figure 9. The effect of extending the individual chirp sections to ensure continuity is shown by the two peaks on figure 9 at approximately the frequencies of the breakpoints – 4Hz and 7Hz.

It can be seen from figure 9 that the power input across the three frequency bands is more equally distributed than for the constant amplitude three section chirp. This power distribution has been achieved by manipulation of the amplitude levels of the three chirp sections for pre-determined sweep rates and frequency breakpoints. This concept will now be extended to define more flexible linear chirp signals with any given variations of power and amplitude with frequency.
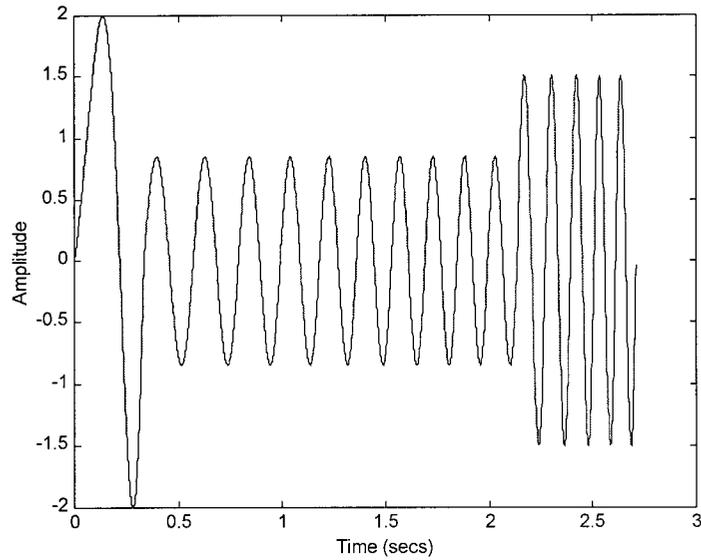
Figure 8 – Three section variable amplitude linear chirp signal
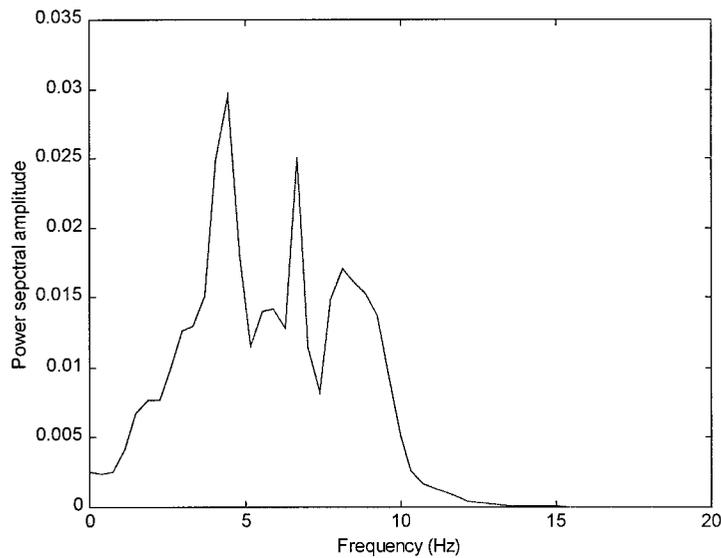
Figure 9 – Power spectrum of three section variable amplitude linear chirp signal

2.3 Multi-section amplitude and power variable non-linear chirp

Whilst the multi-section amplitude variable chirps above allow some control over the energy input within different frequency bands, setting the sweep rates and amplitudes for each chirp section is a matter of trial and error. A more robust system would allow the user to specify the frequency bands, amplitude levels and relative power levels required in each band. The sweep rates and chirp lengths needed to achieve these parameters would then be calculated and a chirp signal derived that ensured continuity and periodicity in the time-domain.

The multi-section amplitude and power variable non-linear chirp described in this work allows the

12

derivation of chirps as described above. In this technique, only the overall chirp length is specified whilst the amplitude is allowed to vary linearly between frequency breakpoints. A non-linear frequency sweep rate is required within each section to allow the specified relative powers and near-linear power variation across each section to be achieved.

A general chirp signal may be expressed as

$$x(t) = A(\omega)\sin\phi(t) \tag{7}$$

where $\phi(t)$ is the instantaneous phase. For a total time duration of T, the Fourier transform of the chirp signal is given by

$$X(\omega) = \frac{1}{T}\int_0^T A(\omega)\sin\phi(t)\, e^{i\omega t}\, dt \tag{8}$$

The autopower spectrum of the chirp is thus given by

$$P(\omega) = |X(\omega)|^2 \tag{9}$$

Thus the aim of this technique is to calculate $\phi(t)$ given $A(\omega)$ and $P(\omega)$. No obvious closed form analytical solution exists for this problem. Instead an approximation will be used whereby the frequency range is divided into a large number of small sections of equal frequency interval and a constant sweep rate is assumed within each section. By calculating the sweep rate and time for each interval, the entire non-linear chirp may be generated from the individual sections with a continuous amplitude and rate of change of amplitude. As a first approximation, however, the sweep rate, power and amplitude of each section may be considered to be constant.

For a typical chirp interval of unknown duration T_j and sweep rate α_j, and known amplitude A_j and autopower P_j, the mean modulus spectrum level for a linear chirp has been evaluated [6], as

$$|X(\omega)| = \frac{A_j}{\sqrt{2}}\sqrt{\frac{\pi}{\alpha_j}} \tag{10}$$

For the jth interval, the contribution to the power at the mean frequency is therefore given by

$$P_j = \frac{\pi A_j^2}{2\alpha} \tag{11}$$

The relative power and amplitude between the jth and k^{th} intervals can be determined from the specification of the chirp. Therefore, using equation (11) it may be seen that

$$\frac{\alpha_j}{\alpha_k} = \frac{\left(\dfrac{P_k}{P_j}\right)}{\left(\dfrac{A_k}{A_j}\right)^2} \tag{12}$$

Each of the intervals, by definition, covers an equal frequency increment. Thus the duration of each interval t_j will be inversely proportional to its sweep rate and it may be seen that

$$\frac{t_k}{t_j} = \frac{\alpha_j}{\alpha_k} \tag{13}$$

Combination of equations (12) and (13) allows the relative time length of each interval to be expressed in terms of the relative power and amplitude levels. As the total time duration of the signal T is specified, it may be seen that

$$\sum_{j=1}^{N} t_j = T \tag{14}$$

such that

$$t_1\left(1 + \sum_{j=2}^{N} \frac{t_j}{t_1}\right) = T \tag{15}$$

Hence, t_1, and subsequently all t_j, may be estimated from the initial specification using equations (13) and (15). Finally, using the known start and end frequency of each interval, the corresponding sweep rates may be found. The required chirp signal is then constructed from the separate chirp intervals, using the methods described earlier to ensure continuity.

14

2.4 Practical Application

It has been shown how a continuous chirp signal may be generated to a specified set of amplitude levels and relative power levels, and with a pre-defined total time duration. One of the prime reasons for customising an input signal for use in vibration testing is to ensure that the rate and amplitude restrictions of the device used to apply the input are not exceeded. Clearly, for a chirp signal, the time-domain amplitude of the input may be specified in advance and thus need not exceed any given limits. Using equation (7), it may be seen that the rate of change of the chirp signal is a cosine function of the instantaneous phase and can therefore also be evaluated and checked for compliance with the excitation equipment.

The primary reason, then, for customising a chirp input signal is to improve the noise-to-signal ratio of the response signal on the understanding that this process will improve the final modal parameter estimates. For a sinusoidal response signal, the best approach to reducing the NSR is to force the response to occupy a greater proportion of the available data acquisition range. In effect, frequency regions of low response amplitude should be driven harder to increase the response levels and resonant regions driven less hard to equalise the response amplitudes across the length of the signal. However, for a constant sweep rate, this approach implies a low level of power input in resonant regions and a subsequently poor NSR on the input signal in the critical areas. Instead, the methodology described above should be used to equalise the power input across the frequency range by varying the sweep rates of the chirp intervals. An example of this approach is given in the next section.

2.5 Simulated Results

Figure 10 shows the Frequency Response Function for a simulated three degree of freedom (DoF) system with natural frequencies of 10, 15 and 16 Hz. A simple linear chirp between 1 and 25 Hz is selected for excitation of this system. The unit amplitude chirp is shown in figure 11 with the corresponding power spectrum shown in figure 12.
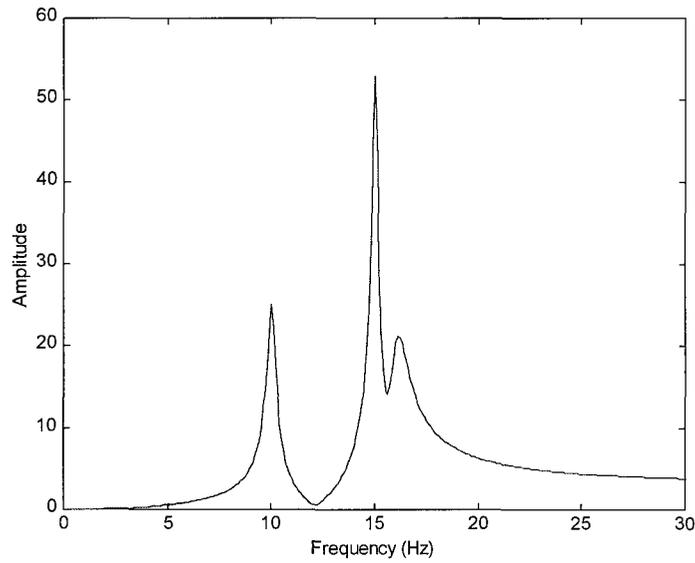
Figure 10 – FRF of simulated three degree of freedom system
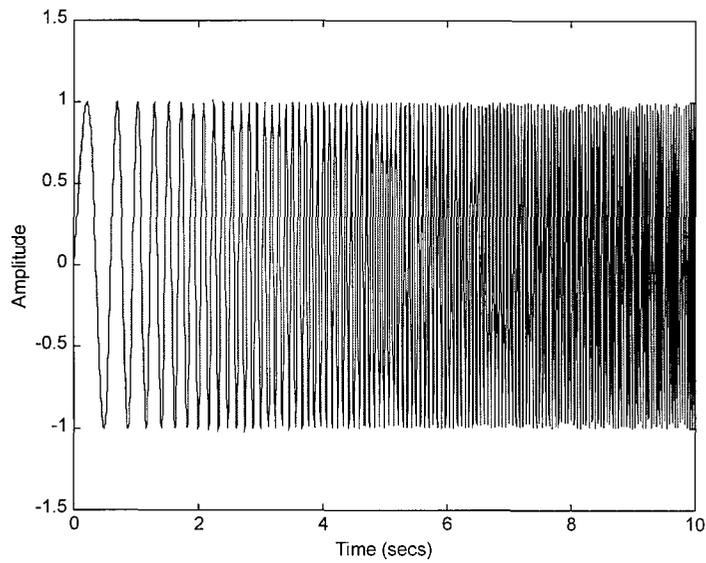
Figure 11 – Linear chirp input signal, unit amplitude
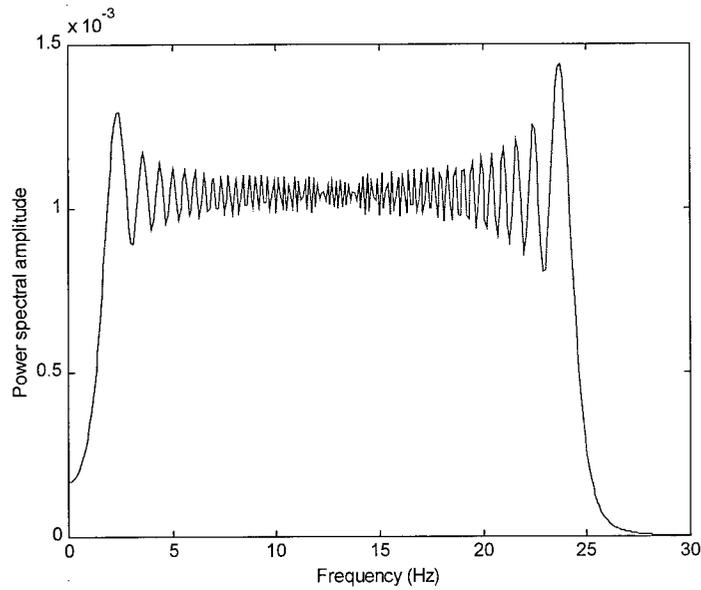
Figure 12 – Power spectrum of linear chirp input signal
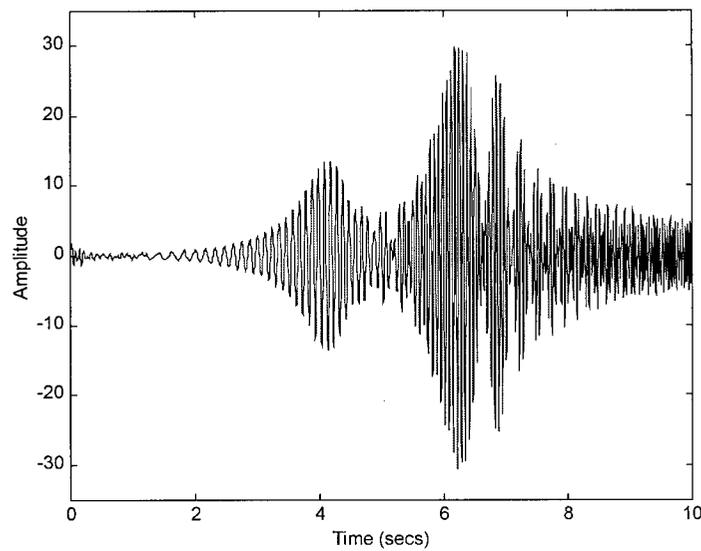
Figure 13 – Response of system to linear chirp input signal

The response of the system to excitation by the linear chirp signal is shown in figure 13 with the associated response power spectrum shown in figure 14. The RMS (root-mean-square) values of the input and response signals are, respectively, 0.7067 and 7.0282.

In order to improve the quality of the parameter estimates resulting from the chirp response data, it is required to reduce the noise-to-signal ratio of both the input and response signals. It will be assumed that the response of the structure is to be held to within the amplitude limits of the initial tests with the linear chirp; scaling of the input signal may be performed at any time to cause the

17

response to occupy the available amplitude and/or data acquisition ranges. However, a certain amount of flexibility will be allowed in the amplitude of the input signal. In essence, it is assumed that the amplitude of the initial linear chirp was defined as that which would provide the maximum allowed response amplitude levels. The aim of the analysis is to re-define the input signal, in terms of amplitude and/or sweep rate, in order to increase both the power input in the important frequency ranges and the overall noise-to-signal ratios, without exceeding the pre-defined response amplitude limits. It should be noted that, throughout this report, the dynamic systems under test are assumed to be linear, such that a doubling of the input amplitude will simply double the response amplitude at all frequencies of interest.
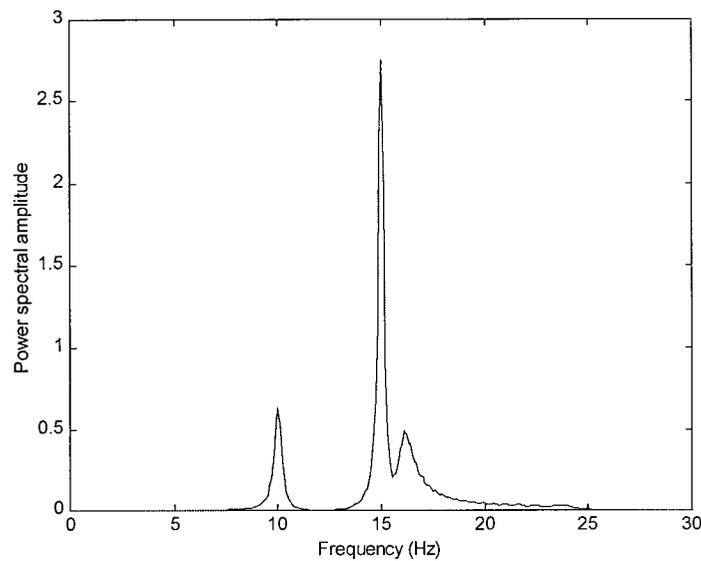
Figure 14 – Power spectrum of system response signal

A three-section variable amplitude chirp signal is shown in figure 15. This signal has been defined as described in the previous sections, with a nominally uniform power distribution across the frequency range 1 – 25 Hz, but with a linear amplitude variation between the breakpoints. The signal is defined to sweep quickly through the low frequency range 1 – 8 Hz with a high amplitude to induce a more significant response level than seen for the original linear chirp. The amplitude is then reduced through the frequency range 9 – 17 Hz, with a minimum level corresponding to the modal frequency at 15 Hz. This section of the chirp uses a slower sweep rate to guarantee the power input in this important frequency range, whilst the low amplitude input ensures that the overall noise-to-signal ratio of the response signal is minimised. Finally, the chirp increases in amplitude through the remaining frequency range. The RMS value of the variable amplitude chirp is 2.3848, more than three times that of the linear chirp, thus implying a threefold reduction in the input noise-to-signal ratio.

The power spectrum of the three-section chirp input is shown in figure 16. It can be seen that the linear amplitude variations enforced upon the chirp cause the power spectrum to vary from its initial

18

uniform distribution. It is believed that lengthening each of the chirp sections to ensure continuity of the signal is responsible for the minima in the power spectrum at 8 and 17 Hz. This effect is similar to that seen during the 'sweep-up /sweep-down' testing approach discussed previously.
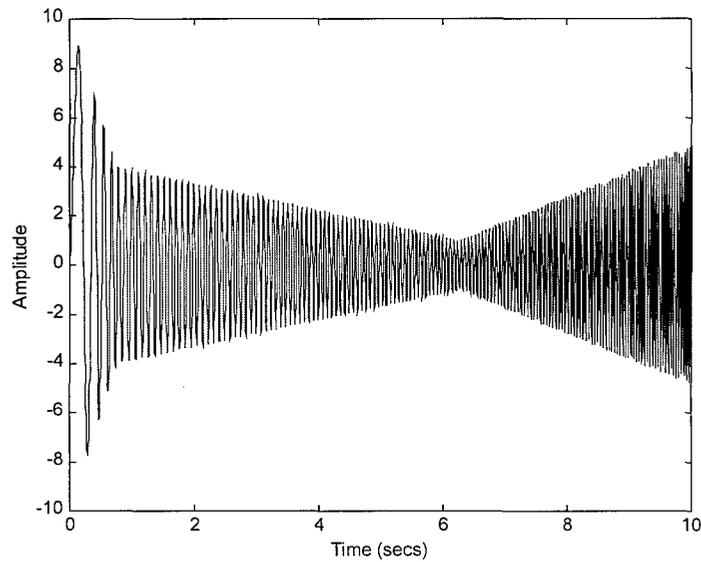
Figure 15 – Three section variable amplitude chirp signal
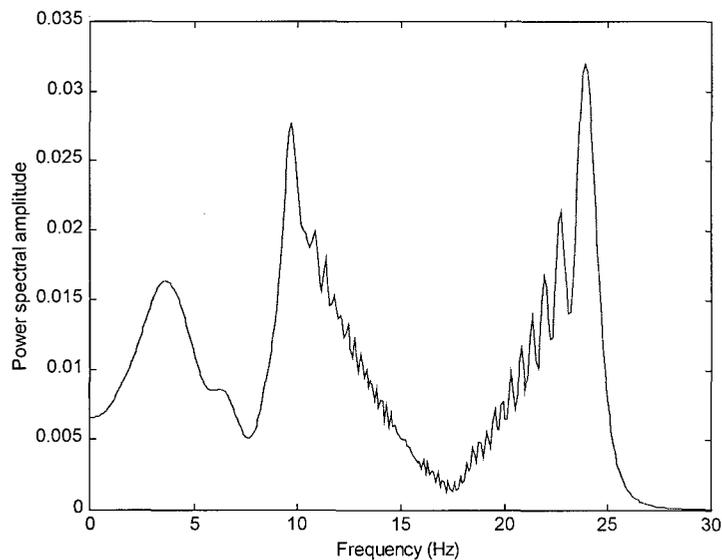
Figure 16 – Power spectrum of variable amplitude chirp signal

The response of the system to the three-section variable amplitude chirp input is shown in figure 17. The RMS value of the response is increased to 9.9343, whilst its maximum value is no greater than that resulting from the initial linear sweep. For any fixed level of additional noise corruption of

the data, the noise-to-signal ratio will thus be reduced. The increase in response power at the important modal frequencies is seen by comparing the response power spectrum for the amplitude variable chirp input, shown in figure 18, to the original response spectrum in figure 14.
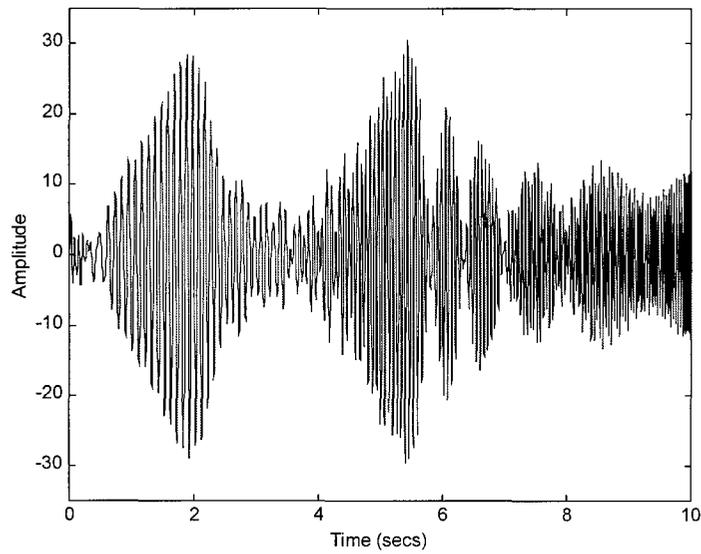
Figure 17 – System response to variable amplitude chirp signal
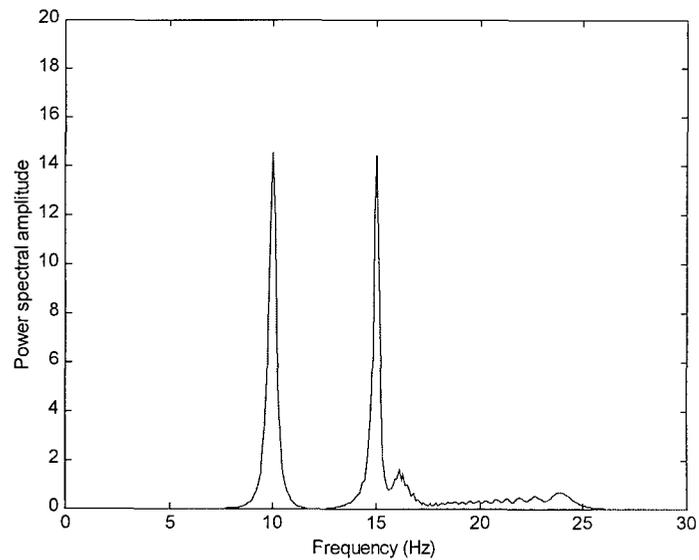
Figure 18 – Power spectrum of system response signal

3. Optimal Random Excitation

3.1 Crest Factor Reduction

Random noise signals are commonly used as input signals in a range of vibration testing applications. However, the nature of such signals means that large positive or negative spikes are likely to occur somewhere within the signal. In order that all of such signals may be used as excitation, both the input amplitude and/or data acquisition range will be scaled accordingly. As a result, the overall noise-to-signal ratio of random signals in real applications is unnecessarily poor.

The crest factor c of a random signal $x(t)$ is defined by

$$c = \frac{\max(x) - \min(x)}{2\sigma_x} \tag{16}$$

Here, σ_x is the standard deviation of $x(t)$ given by

$$\sigma_x^2 = \int_0^T \left(x - \bar{x}\right)^2 dt \tag{17}$$

where $\bar{x}$ is the estimated mean of $x(t)$. For a discrete signal, the standard deviation may be estimated using

$$\sigma_x^2 = \frac{1}{N}\sum_{j=1}^{N}\left(x_j - \bar{x}\right)^2 \tag{18}$$

Sometimes the crest factor is defined in terms of the RMS level of the signal rather than the standard deviation on the assumption of a zero-mean signal. Thus, it may be seen that a signal with a lower crest factor (reduced or eliminated spikes) will yield a lower noise-to-signal ratio in practical applications. In this section, a procedure will be described for reducing the crest factor of any random signal whilst retaining exactly the original power spectrum.

3.1.1 Gerchberg-Saxton Algorithm

The Gerchberg-Saxton algorithm is the most commonly applied technique for crest factor reduction in random signals. This approach utilises a time-frequency clipping method to determine the optimal phase distribution for some pre-determined amplitude and frequency content.

The Gerchberg-Saxton algorithm follows the steps illustrated in figure 19. Firstly, the time signal is

21

clipped at some level between its peak and RMS amplitudes. In practice, all of the points of the discrete time signal above the clipping level are reduced to this level. Similarly, those below the negative clipping level are increased. The optimal level at which to clip the signal has been considered by a number of researchers. Suggested levels include both fixed and variable percentages of either the maximum amplitude or the $\sqrt{2}$ times the RMS level. It is generally accepted that the signal should be clipped below the required maximum amplitude to aid a rapid convergence of the algorithm. However, clipping at too low a level can actually result in longer times to convergence or, in extreme cases, unstable oscillations of the signal between successive iterations of the algorithm.

Following the clipping of the time-domain signal, the resulting signal is Fourier transformed. A new frequency-domain signal is then created from the amplitude spectrum of the original signal and the phase of the clipped signal. The inverse Fourier transform yields the updated time-domain signal which is clipped at the beginning of the next iteration. The process may be halted when the crest factor of the signal falls below a pre-specified value or when the reduction of the crest factor is no longer significant with further iterations (i.e. convergence).

A simple implementation of the Gerchberg-Saxton algorithm is shown in figures 20 – 22. Figure 20 shows a broadband random signal with a uniform input spectrum, and a crest factor of 3.31. Application of the Gerchberg-Saxton algorithm causes the crest factor of the signal to drop, as illustrated in figure 21. The final signal, shown in figure 22, has a crest factor of just 1.49 but with the same amplitude spectrum as the initial signal. In this case, the crest factor reduction was halted as soon as a value below 1.5 had been achieved.
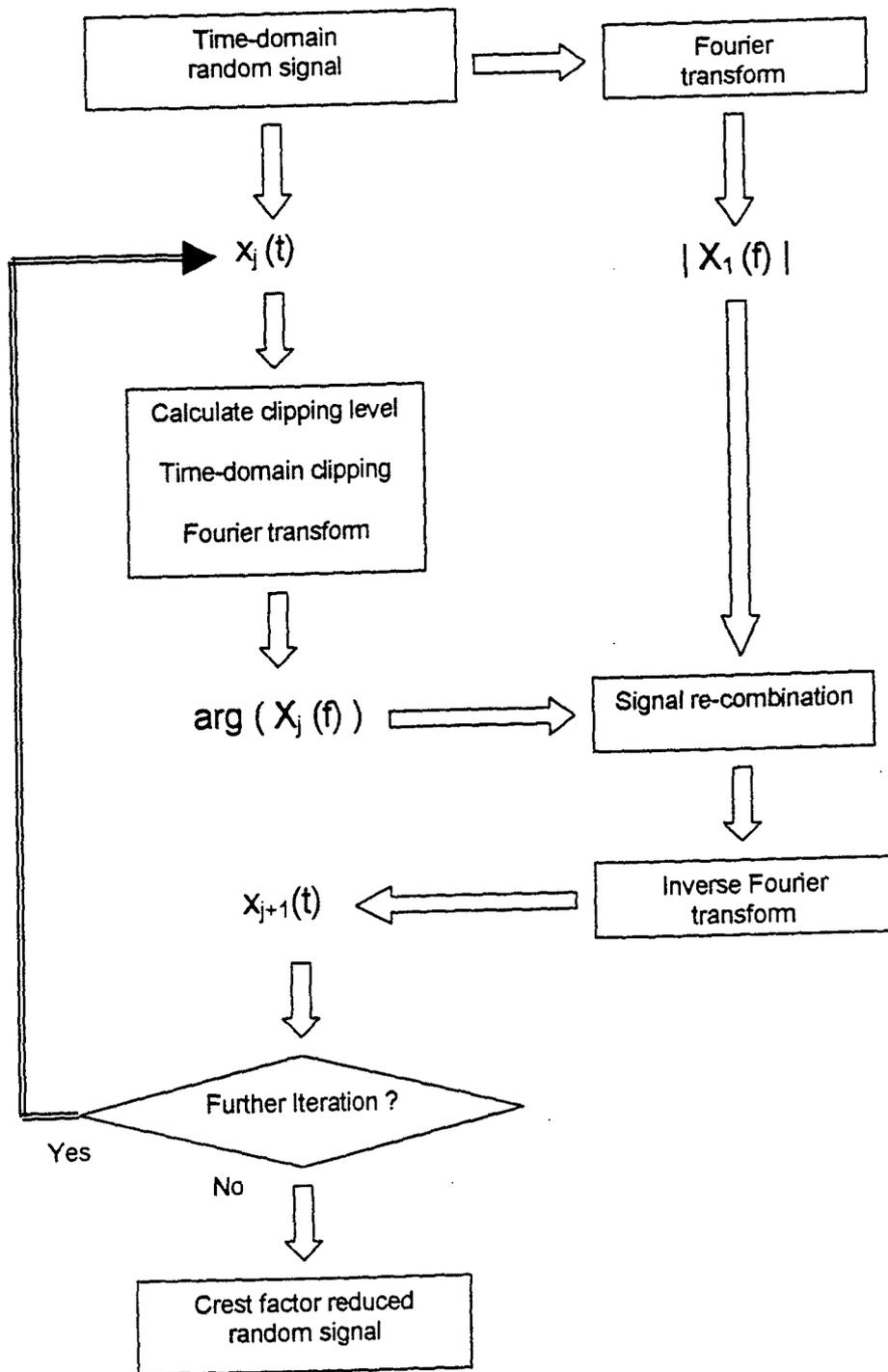
Figure 19 - Gerchberg-Saxton Flow Diagram
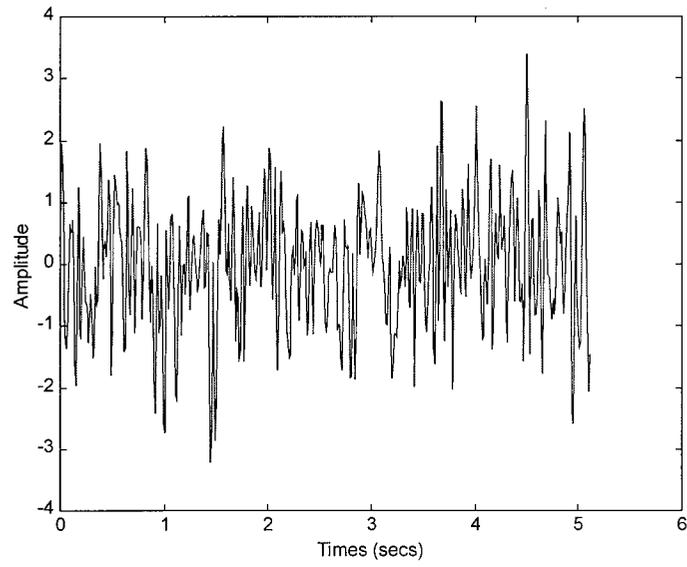
Figure 20 – Broadband random signal
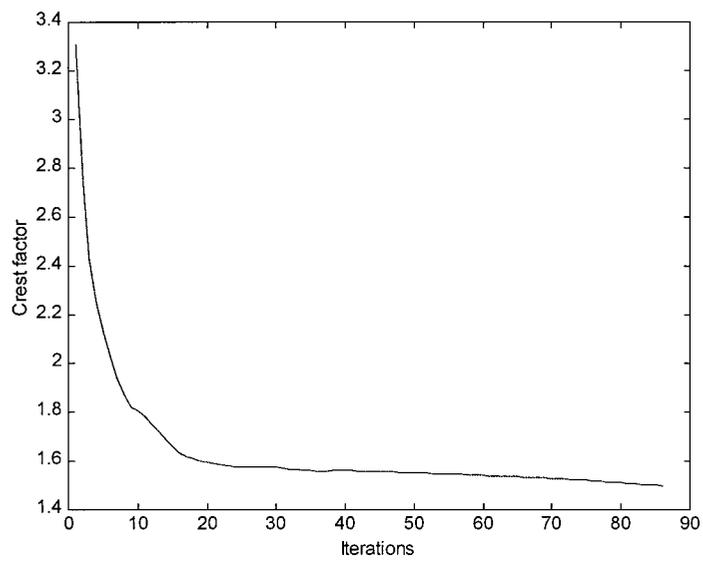
Figure 21 – Progress of Gerchberg-Saxton Algorithm
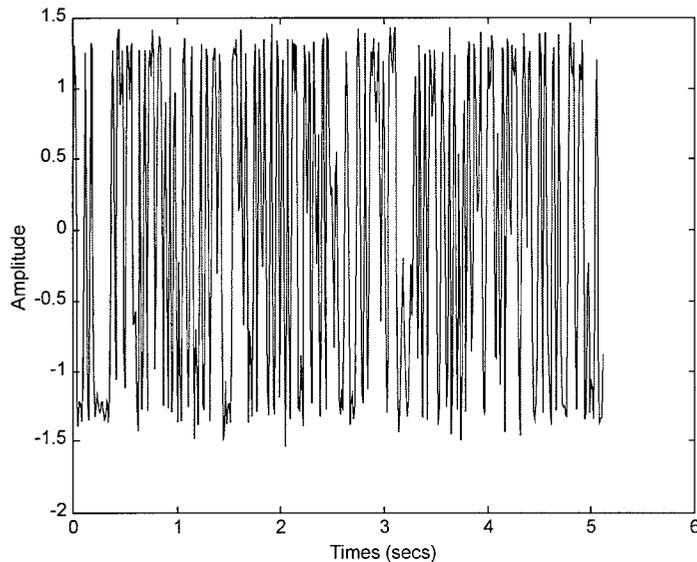
Figure 22 – Crest factor reduced broadband random signal

3.1.2 Snowlines

In the previous example, based on the Gerchberg-Saxton algorithm, the initial amplitude spectrum is re-imposed upon the clipped signal. However, in many applications, only sections of the frequency range need to be specified exactly, allowing some flexibility in the frequency content of the final signal for the remaining frequencies. By allowing these non-critical frequency components, known as 'snowlines', to take other values, it has been seen that crest factor reduction can be performed more efficiently.

A simple example of the use of snowlines for crest factor reduction involves a band-limited random signal, as illustrated in figures 23 and 34. The amplitude spectrum is defined to be uniform for the lower half of the frequency range; the remainder is initially set to zero. However, as the upper frequency range is non-critical, any values will be accepted this region. The Gerchberg-Saxton algorithm is then implemented, but with only the lower half of the frequency range reset every iteration. Figure 25 shows the progress of the algorithm as the crest factor is reduced. The final signal has a crest factor of 1.47 as compared to the initial value of 3.15, whilst the reduction only took eight iterations. Although the signals used in this and the previous simulation are different and cannot be directly compared, the significant reduction in the number of iterations required is typical of the use of snowlines. The final signal is shown in figures 26 and 27, in which the non-zero snowlines of the upper frequency range are apparent.

The use of snowlines thus reduces the number of iterations required for a given level of crest factor

reduction and may be used in situations where only specific frequency regions of the input spectrum need to be retained. The use of snowlines is more fully investigated in [7]. An interesting result of this work is that, as the number of non-zero spectral lines is reduced, the resultant time-domain signals tend towards chirp-like signals. As chirps are sinusoidal, they exhibit the minimum possible crest factor value of $\sqrt{2}$. The implication of this result, then, is that the random signal with the absolute minimum crest factor is actually a chirp signal whose sweep rate is altered to give the required amplitude spectrum. Further work in this are is required to integrate the results of chirp and random signal optimisation.
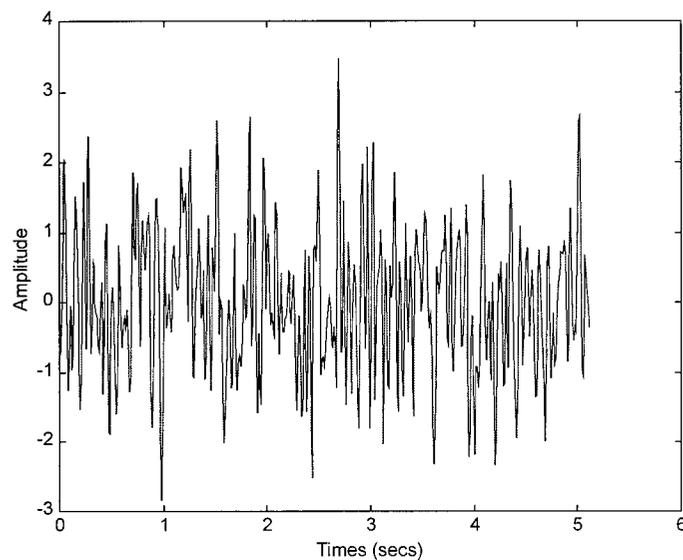
Figure 23 – Narrowband random signal
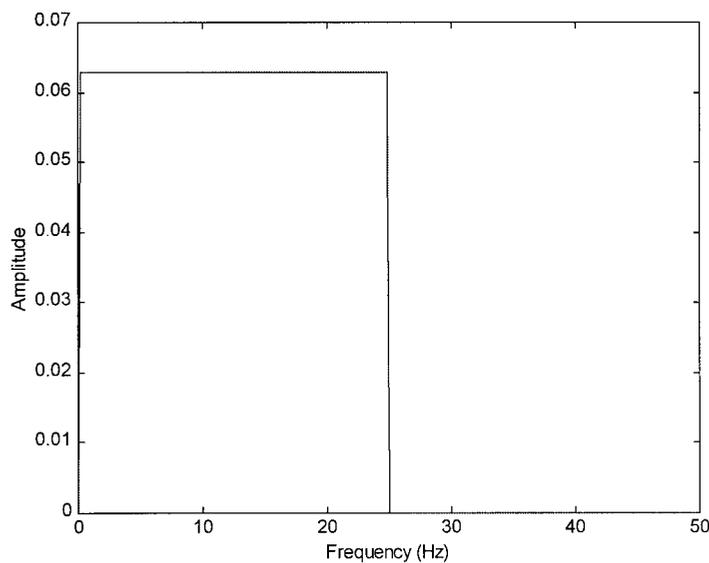
Figure 24 – Amplitude spectrum of narrowband random signal

26
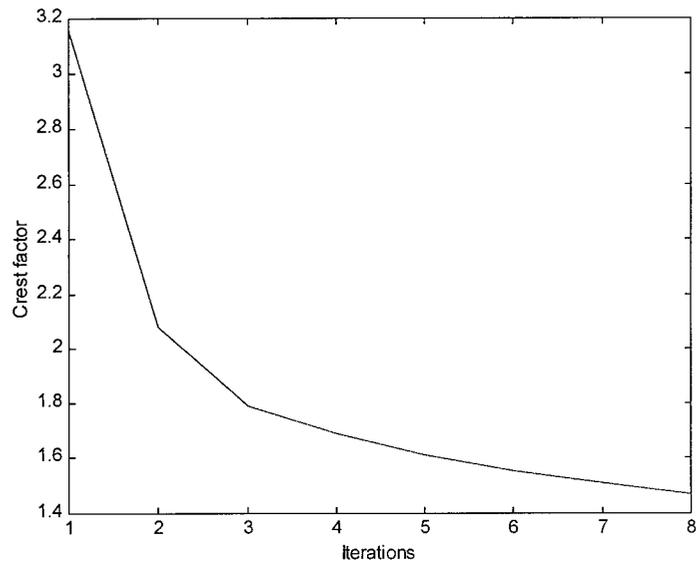
Figure 25 - Progress of Gerchberg-Saxton Algorithm
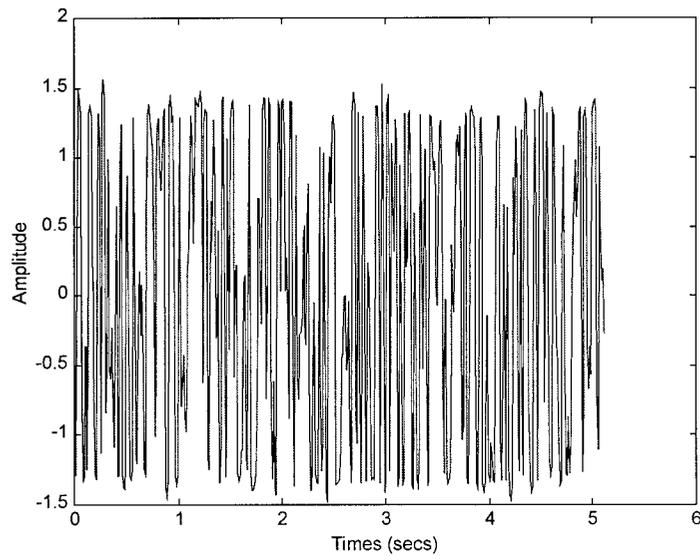
Figure 26 – Crest factor reduced narrowband random signal
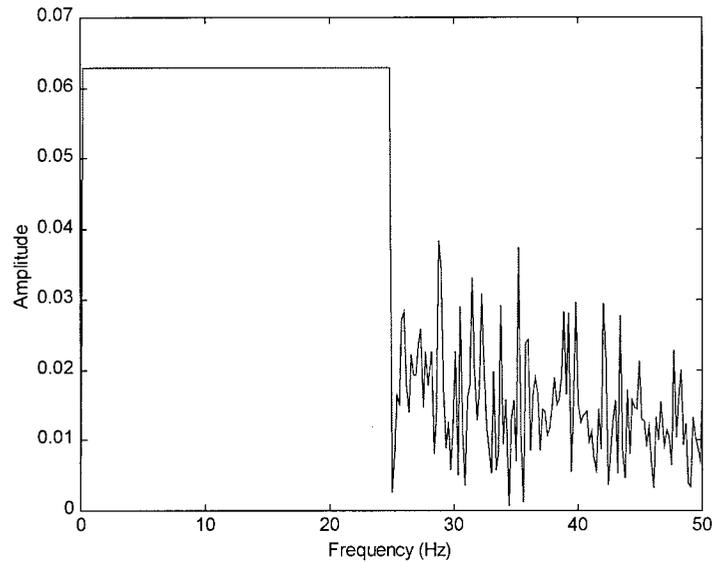
Figure 27 – Amplitude spectrum of crest factor reduced narrowband random signal

3.1.3 Other Considerations

The Gerchberg-Saxton algorithm, and the examples given above, simply take a random signal and reduce the crest factor, thus tending to reduce the noise-to-signal ratio of the signal in practical applications. However, if the crest factor reduced signal is to be used as input for the purposes of vibration testing, other practical factors need to be taken into consideration. Specifically, the maximum rate and amplitude levels of the excitation device will limit the input signals which may be applied physically to a structure. Excitation signals which would require higher rate and/or amplitude levels than are possible with the given device would not be applied correctly. Instead, the applied force would appear clipped or time-lagged with respect to the input signal, with consequent distortion of the input frequency characteristics. The second consideration is the noise-to-signal ratio of the response signal, which is as important as the input signal in terms of the accuracy of the derived modal parameters. Clearly, however, an input signal with the minimum crest factor will not lead to a response signal with a similarly low crest factor. In order to optimise the crest factors in both the input and response signals, the transfer function of the system needs to considered within a two-stage optimisation process. A similar procedure may be used to account for maximum amplitude and rate considerations.

In terms of crest factor reduction for both input and output signals, the simplest approach is a two-stage implementation of the Gerchberg-Saxton algorithm. For an input-output optimisation to be performed, an estimate of the system Frequency Response Function is required, from either a previous test or a numerical model. Firstly, the Gerchberg-Saxton algorithm is first applied to the input signal for one iteration and the crest factor calculated. Next, the predicted response of the

system to this input is estimated and the crest factor of this signal reduced by again applying one iteration of the Gerchberg-Saxton algorithm. The improved response signal is then inverse-filtered using the estimated Frequency Response Function to yield the corresponding input signal. The inverse-filtering procedure is best performed in the frequency domain to avoid problems of minimum phase. The two-stage Gerchberg-Saxton algorithm described then iterates, consecutively reducing the crest factor of the input and output signals until some criteria is met.

Simple criteria based on limits and/or convergence may be specified in terms of both the input and output crest factors. However, as the crest factor is essentially a statistical measure – the range of the data set normalised by twice the standard deviation – simple statistical analysis suggests a form for a combined crest factor from two signals. Given signals $x_1(t)$ and $x_2(t)$ with corresponding individual crest factors c_1 and c_2, then the combined crest factor c_{tot} will be defined as

$$c_{tot} = \sqrt{c_1^2 + c_2^2}$$

(19)

As the minimum crest factor for any sine-based signal is $\sqrt{2}$, it may be seen that the minimum possible value of c_{tot} will be 2.

The two-stage Gerchberg-Saxton algorithm described will tend to minimise the value of c_{tot} and yield reasonable input and predicted output signals. However, the minimisation procedure may not be achieved optimally in terms of the total computational requirement and variations to the simple scheme described have been suggested. The first option is to run the Gerchberg-Saxton algorithm until convergence on the input signal prior to calculating the response, and then to continue with the crest factor reduction of the input and output consecutively. The aim of this technique is to eliminate a number of the filtering and inverse-filtering operations in the early iterations. However, simple optimisation of the input without consideration of the response may lead to response signals with initially very high values and, ultimately, the necessity for a larger number of iterations. A second option is to concentrate the crest factor reduction at each iteration on the signal with the highest crest factor rather than simply alternating between the input and response signals. This approach has the potential to optimise both signals in fewer iterations. However, as will be seen in the simulation presented, the crest factor reduction of input and response signals are opposing criteria which will tend to cause the algorithm to alternate between the two signals in the later stages of the optimisation anyway.

The two-stage Gerchberg-Saxton algorithm, in its original form, will be demonstrated using the three DoF system FRF shown in figure 10. The initial narrowband random input signal, with a crest factor of 3.12, is shown in figure 28. The response of the system to this input is shown in figure 29 and has a crest factor of 3.10. The algorithm was implemented using snowlines and the individual

and combined crest factors plotted after the crest factor reduction of either signal.
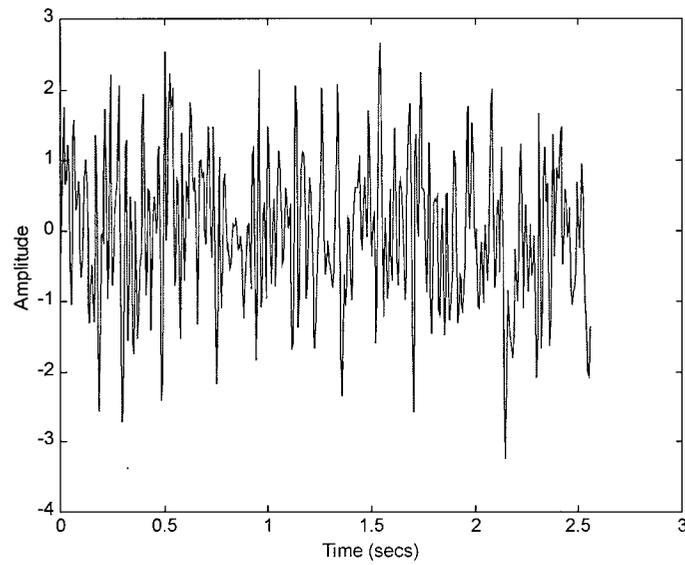
Figure 28 – Narrowband random input signal
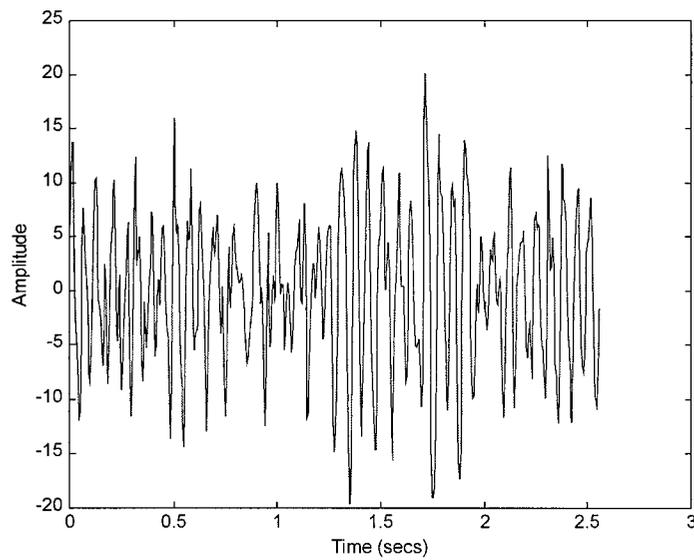
Figure 29 – Response of 3DoF system to random input signal

Figure 30 shows the progress of the two-stage Gerchberg-Saxton algorithm, which shows both the input and output crest factors reducing in consecutive iterations. Clearly, the minimisation of the input and output crest factors are opposing criteria, leading to an oscillation of both traces as the algorithm switches between the two signals. The combined crest factor is reduced from 4.395 to 2.547. In practice, for two random signals linked by a transfer function, the minimum c_{tot} value of 2

is very unlikely to be achieved.
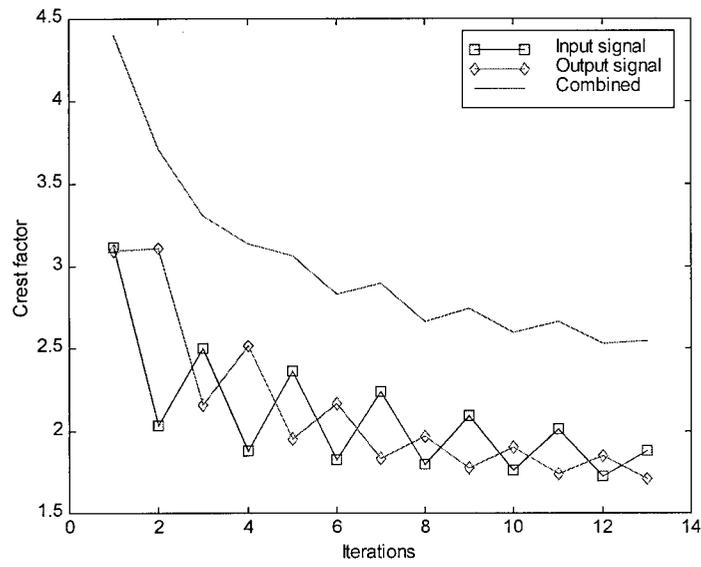
Figure 30 – Progress of two-stage Gerchberg-Saxton algorithm
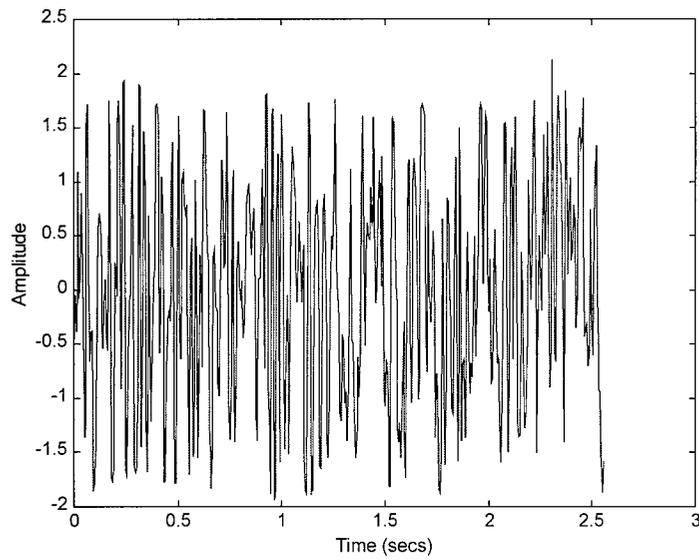
Figure 31 – Crest factor reduced narrowband random input signal

31
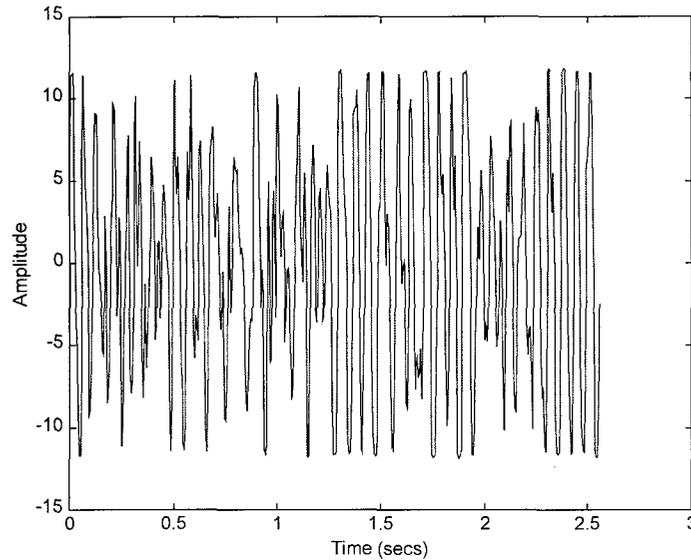
Figure 32 – Response to crest factor reduced random input signal

A simple two-stage implementation of the Gerchberg-Saxton algorithm has been demonstrated for the simultaneous crest factor minimisation of random input and response signals. As discussed above, a practical requirement of crest factor reduced signals is that neither the maximum rate nor amplitude of the exciter is exceeded. Thus, a need exists for simultaneous displacement and velocity crest factor reduction to ensure that low noise-to-signal ratios are obtained within the limitations of the given excitation device. For sine-based signals, the relationship between the displacement and velocity is given by the simple frequency domain transformation

$$\dot{x}(\omega) = i\omega\, x(\omega) \qquad (20)$$

Hence, the displacement-velocity crest factor optimisation may be undertaken in exactly the same way as for input-output signals, using a transfer function of $i\omega$ in the two-stage Gerchberg-Saxton algorithm. Figure 33 shows the progress of a two-stage Gerchberg–Saxton algorithm for the simultaneous reduction of amplitude and rate crest factor, applied to a narrowband signal with the inclusion of snowlines. For both signals, clipping was performed at a percentage of the instantaneous RMS level rather than at some pre-defined level corresponding to a physical limit. Figure 33 shows the displacement crest factor reduced from 2.61 to 1.57 and the rate from 2.92 to 1.40 in 53 iterations. The combined crest factor thus drops from 3.91 to 2.10. In both the amplitude and rate signals, a significant reduction is seen in the maximum values.

Clearly, simultaneous crest factor reduction may still not yield compatible displacement and velocity signals in terms of the physical limits of the excitation device. Instead, the inputs may be scaled to fit the most restrictive of the limitations, with the wasted capacity in terms of the other parameter

32

accepted. Alternatively, the crest factor reduction may be focused on the signal which is closest to its physical limits at each iteration thus exploiting the flexibility in the other parameter. In this way, simultaneous crest factor reduction of the displacement and velocity components of a single signal may be used to ensure the optimum noise-to-signal ratio in both signals within pre-determined limits.
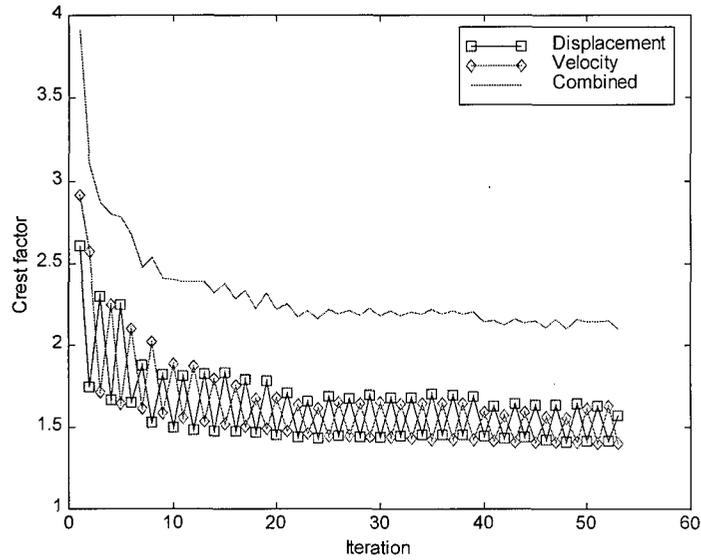
Figure 33 – Progress of two-stage Gerchberg-Saxton algorithm

3.2 Comparison With The Schroeder Phase Approach

Schroeder [10] developed one of the first approaches to devise a phase distribution such that the crest factor of a random signal is minimised. His method was based upon the observation that a Frequency Modulated signal would always possess a low crest factor. With the assumption that the number of harmonic components in the specified power spectrum are large and in a band width that is small compared to the centre frequency, the relationship between the phases Φ

$$\Phi_n = \Phi_1 - 2\pi \sum_{k=1}^{n-1} (n-k)p_k \qquad n = 1,2,\cdots,N$$

is a good choice for a low crest factor signal. p is the power spectrum for each harmonic and N is the total number of harmonics.

The above formulation is further simplified in the special case where the spectra is flat. The results of the above method degrade when the above assumptions are violated which is the case if a wide range frequency range is required. The Schroeder method has been considered by NASA as a possible method of generating random signals for flight flutter testing excitation.

In the following simple example, the displacement clipping and Schroeder methods are compared for the generation of a random signal of 1024 data points, sampled at 40Hz that was required to produce a uniform power spectrum between 1 Hz and 10 Hz.

The Schroeder method has a fixed phase distribution relative to the first harmonic. This first phase was varied for 30 different cases. The clipping approach, however, is dependent upon the initial random phase distribution, and 30 different initial phase distributions were carried out to obtain signals with the same power content. The following results were found

Method	Average Crest Factor	Standard Deviation	Maximum Crest Factor	Minimum Crest Factor
Schroeder	1.818	0.036	1.851	1.732
Clipping Method	1.568	0.023	1.601	1.507

It can be seen that there is a significant improvement in the clipping approach results compared to the Schroeder method, even when the worst of the 30 different cases is taken. These findings were found to hold for a number of different test cases.

4. Statistical Implications

4.1 Introduction

Approaches for the noise-to-signal minimisation of both chirp and random signals have been presented and demonstrated on simulated systems. However, so far only single chirp or random sequences have been considered. In practice, it is known that better power spectra, Frequency Response Functions and subsequent modal parameters may be obtained by using averaging procedures applied to the results of a number of chirp or random excitation tests. For a fixed total test time, a choice must be made between a chirp or a random input. Following this decision, it would be useful to predict whether the results of one long sequence are likely to be superior or inferior to the average of a number of shorter sequences. In order to answer these questions, random and chirp signals must be considered separately in terms of their statistical parameters.

4.2 Random Signals

The statistics of broadband random signals are well understood, and described in depth in [8,9]. For a random signal $x(t)$, sampled every Δt seconds to a give a sequence of N points, the power spectral density (PSD) evaluated from the data will differ from the true PSD which corresponds to the underlying random process from which the data has been drawn. Clearly, the aim is to best approximate the (unknown) true PSD from the available data. The difference between the true and measured PSD derived from a random signal may be characterised by estimates of the variance and bias. Variance is a measure of the random spread of an estimated about its true value; averaging a large number N of similar estimates will reduce the variance as a function of $1/N$ to the limit of zero variance when an infinite number of results are averaged. In comparison, bias is an offset of the expectation of the estimated parameter which cannot be removed by averaging. In many statistical applications, a trade-off exists between bias and variance of results for a fixed quantity of data.

Expressions exist [9] for the variance and bias of estimated PSDs based on averages from n independent random sequences. It should be stressed that the variance and bias described here relate only to the approximation of the PSD by a finite number of data samples and are completely unrelated to any additional noise corruption of the measured data. For the estimated autopower spectrum, $\hat{G}_{xx}$, the variance σ_{xx}^2 is given by

$$\sigma_{xx}^2 = \frac{G_{xx}^2}{n} \tag{21}$$

For the crosspower spectrum between samples of $x(t)$ and $y(t)$, the variance σ_{xy}^2 is given by

$$\sigma_{xy}^2 = \frac{\left|G_{xy}^2\right|}{\gamma_{xy}^2 n} \tag{22}$$

where γ_{xy}^2 is the coherence between the signals $x(t)$ and $y(t)$. It is clear, then, that the variance of the spectral estimates decreases as the number of averages used is increased.

The bias on a power spectral estimate G_{xx} may be approximated by

$$b(G_{xx}) = \frac{1}{24T^2} \frac{\partial^2 G_{xx}}{\partial \omega^2} \tag{23}$$

where T is the total time length of the averaged sample. The bias is thus a function of the curvature of the power spectrum at frequency ω, giving a maximum at spectral peaks, and is inversely related to the square of the sample length. As the frequency resolution is dependent upon the sample length, the bias error may be viewed in terms of the spacing of the spectral lines in the frequency domain. As the sample length is reduced, the frequency resolution becomes worse such that the energy from a wider frequency band is represented by a value at each single frequency line. Clearly, as the resolution becomes worse the estimated PSD values are increasingly inaccurate estimates of the true PSD at each frequency. The degree of inaccuracy is then related to the curvature of the PSD across the frequency band, as givne by equation 23.

In practice, it is difficult to accurately evaluate the bias as given in equation 23. However, if a simple single DoF system is assumed, it can be shown that the bias is essentially negligible for sample lengths which give a frequency resolution of less than 0.25 times the half power bandwidth of the spectral peak. This analysis may be applied to well-separated peaks in the power spectra of multiple DoF systems.

For a fixed test time length, $T_{tot} = nT$, a clear trade-off is presented between minimisation of the variance and bias errors of the estimated spectra. The question of whether it is better to use a single random sequence or the average of a number of segments thus depends upon the respective levels of variance and bias error which are deemed acceptable.

Figure 34 shows the response power spectrum of the three DoF system described earlier, when excited with a single, 8192 point broadband excitation signal. The variance of the estimated PSD (solid line) is clear with respect to the true PSD (dashed line). Repeat tests would show a similar level of variance, but with a different specific error on each spectral line. Figure 35 shows the response PSD as estimated from the average of 16 segments of 512 points. Clearly, the variance

of the PSD estimate is greatly reduced. However, the estimated PSD values shown by the diamonds do not correspond to the true PSD due to the bias error, now significant as a result of the poor frequency resolution. Repeating this test would return PSD estimates with the same levels of bias on each spectral line. It should be noted that the linear interpolation between the estimated points of figure 35 is purely for display purposes – the estimates are only valid at the points indicated by the diamonds.
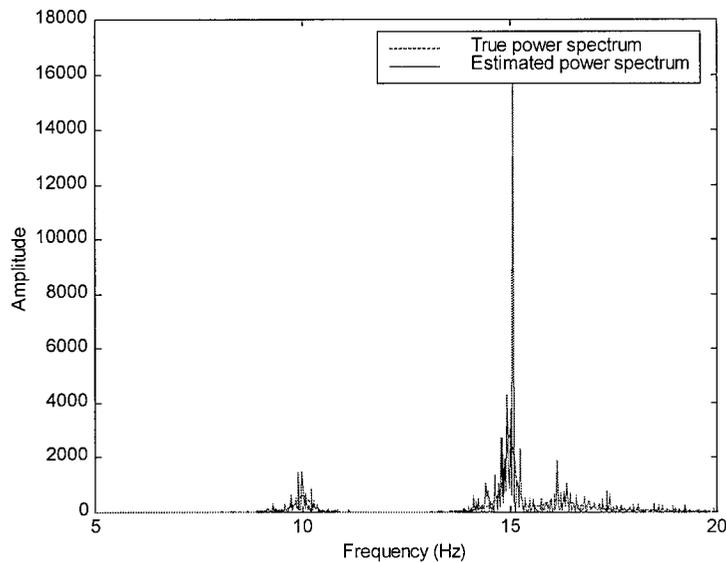
Figure 34 – Power spectrum resulting from a single random input signal
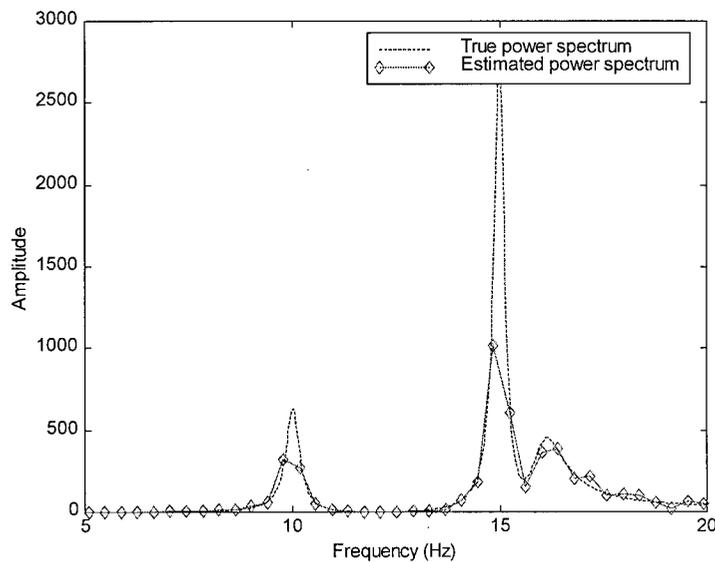
Figure 35 – Power spectrum resulting from an averaged random input signal

For subsequent analyses, neither of the results shown above would be ideal. A compromise based on four averages may be more suitable. A common technique which can yield additional information is the use of overlap averaging. In this procedure, overlapping segments are averaged

37

such that some elements of the time-domain signal are used more than once. For example, consider 4096 point data set on which averaging is to performed to yield a 1024 point set. With zero overlapping, four separate 1024 point segments would be taken – starting at points 1, 1025, 2049 and 3073 respectively - and averaged. However, if 50% overlap is used, seven 1024 segments may be defined, starting at points 1, 513, 1025, 1537 ... 3585, such that the majority of the total signal is included in two of the seven segments. In general, the number of segments which may be averaged using overlap techniques, n_{over}, is given by

$$n_{over} = \left(\frac{T_{tot}}{T} - 1 \right) \left(\frac{1}{1 - u/100} \right) + 1 \qquad (24)$$

where T is the time length of each sample, T_{tot} is the total time length of the test data set and u is the overlap percentage.

The application of overlap averaging is well known. However, the apparent increase in the number of averaged samples with no loss of frequency resolution implies, with reference to equations 21-23, that the variance of the final power spectrum estimate may be decreased with no corresponding increase in bias. Clearly, this cannot be the case. Strictly, the expressions for spectral variance and bias presented above are based upon the assumption of independent random signals. As a result, the degree of overlap averaging cannot be increased indefinitely. However, empirical studies have shown that for overlap levels of up to 66%, an apparent improvement in both variance and bias errors can be achieved with respect to the results of non-overlapped averages.

As mentioned previously, the variance and bias of the estimated power spectra described in this section occur entirely due to the random nature of the signals being used and the approximation of the true underlying power spectra from a finite data set. Such errors do not affect deterministic signals such as chirps. The second, potentially dominant source of error, is that of noise corruption of the data. Such noise will affect any measured signal – random or deterministic – and is generally dealt with as an unknown random sequence. Averaging procedures will tend to decrease the variance of this noise in the frequency domain. Ultimately, however, additional white noise on time-domain signals will result in a bias of estimated power spectra with respect to the uncorrupted spectra required. As a bias, this type of error cannot be eliminated through the use of averaging procedures.

It is finally worth noting that the expressions given for variance and bias, and indeed the discussion of overlap averaging, take no account of any windowing functions which should be applied to all random signals to eliminate leakage errors.

4.3 Chirp signals

As deterministic signals, chirps do not suffer from the variance and bias errors associated with random signals, but are still affected by additional noise corruption of measured data. As a result, the expressions given in the previous section are not valid for chirp signals.

A subtle difference exists between the use of random and chirp signals, namely that segments of a random signal may be averaged on the assumption that the frequency content of each sample is the same as that of the whole signal. For a chirp signal, this is clearly not the case and, if averaging is required, a number of identical, short chirp sequences must be applied sequentially to the system. In practice, the use of very short chirp signals can cause problems as the system under excitation is never truly in a steady state during the test. Also, the use of windowing functions can result in the loss of a significant quantity of information if a large number of short chirp signals are used.

The simulation presented is the previous section is now repeated, using a chirp input signal. For the averaged result, the same, shorter chirp signal was applied to the system. Figure 36 shows the results generated using the full 8192 point chirp, whilst the results of the averaged shorter chirps is shown in figure 37.
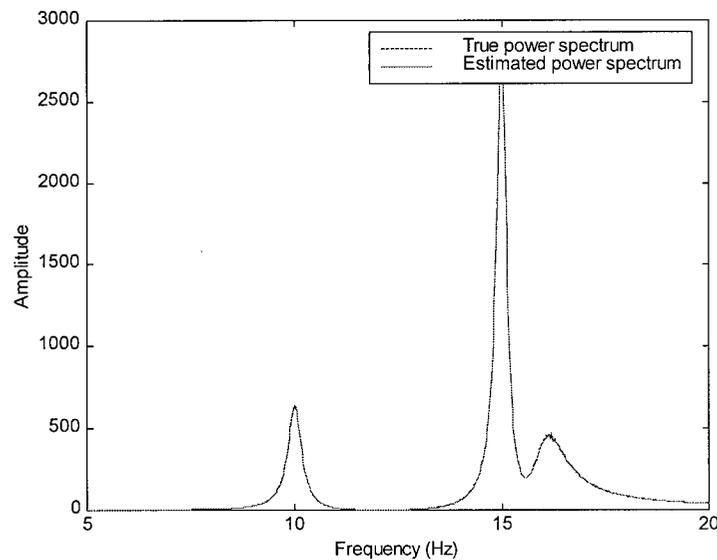
Figure 36 – Power spectrum resulting from a single chirp input signal
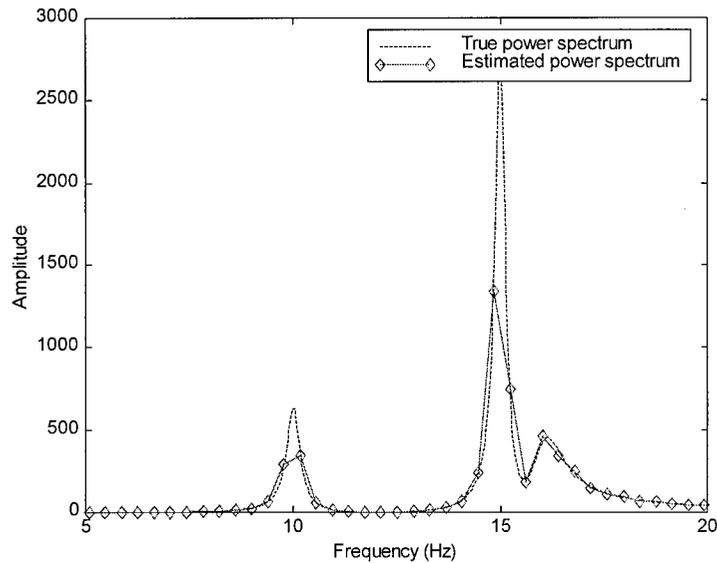
Figure 37 – Power spectrum resulting from an averaged chirp input signal

Clearly, in the absence of the estimation errors related to random signals and additional noise, the results of the single chirp input seen in figure 36 give a perfect match to the true power spectrum. Equally, the results of the averaged multiple chirp inputs, shown in figure 37, are very good, although the frequency resolution is arguably too low for accurate parameter estimates to be obtained. Therefore, for a noise-free deterministic signal, there is no benefit in averaging and a single long chirp is the best choice from the point of view of frequency resolution.

Averaging can only be of benefit for deterministic signals if the sampled data is corrupted by noise. The above simulation was repeated with the addition a high level of white noise to the response signals. The results are displayed in figures 38 and 39 for the single and averaged chirps respectively. Clearly, from figure 38, using a single long chirp with no averaging leads can lead to badly corrupted power spectra estimates in the presence of noise. Averaging will reduce the variance of the noise, as seen in figure 39, although only at the cost of frequency resolution. The underlying bias effect of the noise on the response power spectrum is also visible in this figure where the estimated spectrum is greater than the true value for the majority of the spectral lines.
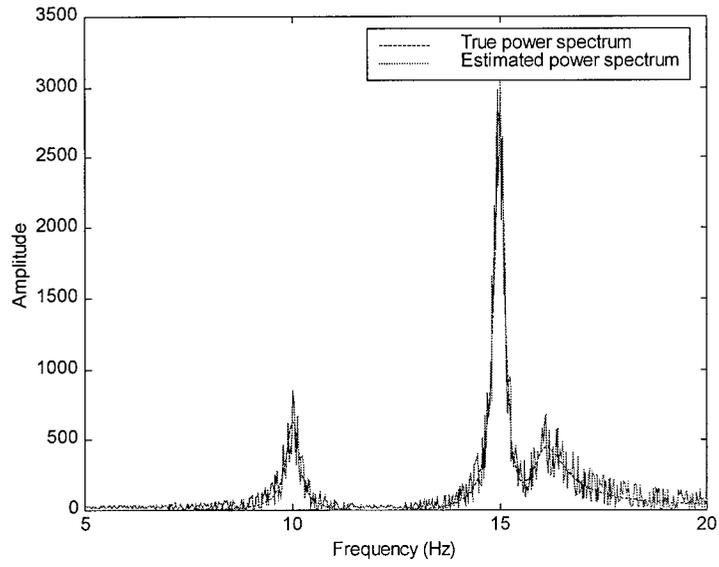
Figure 38 – Power spectrum resulting from a single chirp input signal with noise
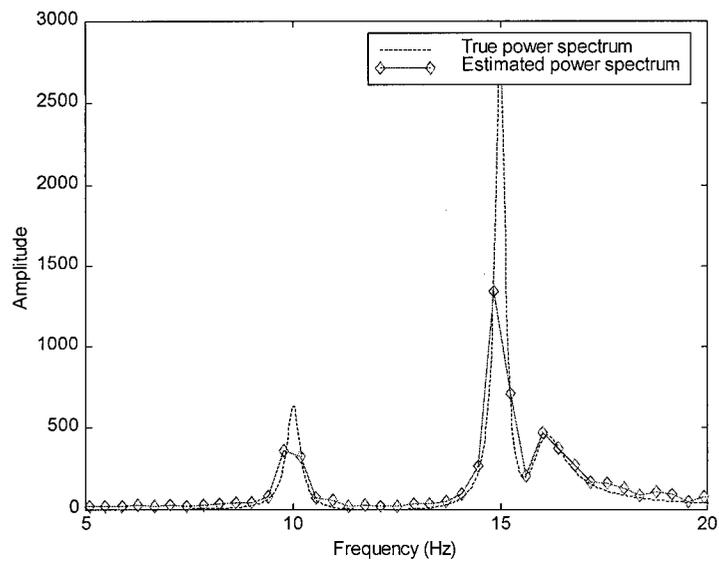
Figure 39 – Power spectrum resulting from an averaged chirp input signal with noise

41

5. Random or Sweep Excitation ?

The methods that have been developed in this work have been shown to improve upon the approaches used currently for the generation of sweep and random excitation signals. One question that is of interest is whether it is better to use sweep or random excitation. Of course, the type of excitation devices available may preclude any choice e.g. the DEI vane is only able to provide steady or step sine excitation signals.

In terms of crest factor, the sinusoidal approaches are always superior to the random signals, and the amplitude at any given point of the input signal can be easily found. Also, if the generated random signals tend towards chirps during the crest factor optimisation process, this would tend to suggest that chirps are the best type of signal. However, the clipping process is solely minimising the crest factor, and not how well the frequencies are 'mixed-up'.

Both chirp and random signals can be formulated to concentrate on frequency regions of interest. The key question to consider is whether it is

1. better to put a lot of energy into a frequency region for part of the time as with a chirp, where there will be a good signal-noise ratio, but a poor one for the rest of the duration of the excitation, or
2. to excite across the entire frequencies of interest – not giving such a strong excitation but also counteracting any noise for the entire duration of the signal.

Aside from arguments regarding the stationary behaviour of the noise, if the random and chirp signals have the same frequency content, then exactly the same results should be obtained. The only difference between the signals is, of course, the phase, which leads to differences in the crest factor. If it is possible to tune the gains for the chirps such that the maximum amount of energy can be put in without overload of the excitation or measurement system, then the best results should be obtained using chirp excitation.

42

6. Conclusions

A number of improvements have been proposed to the excitation signals traditionally used during flight flutter testing. The aim of these improvements is to optimise the distribution of energy within a time-domain signal such that noise-to-signal ratios are minimised, and the accuracy of subsequent parameter estimation techniques is improved.

For chirp (sine-sweep) signals, it has been shown that a variable overall sweep rate may be defined, based upon a series of linear sweep-rate variations, which will allow given power and amplitude distributions to be combined within a fixed length chirp signal. Such a signal has been input to a simulated system resulting in reduced noise-to-signal ratios on both the input and response signals.

For random signals, the Gerchberg-Saxton algorithm for crest factor reduction has been described and demonstrated as a method of improving the noise-to-signal ratio. This algorithm has been extended to the optimisation of input and response signals, in situations for which a good representation of the system FRF is available, and also for the simultaneous optimisation of amplitude and rate parameters, for cases where physical limits exist in the excitation system.

Simulated studies have been used to demonstrate the application of the proposed methods and to show that they are superior to the conventional random generation or linear sweep approaches. The statistical aspects of averaging with the new methods have been considered and, as would be expected, the use of averaging reduces the effect of noise on the measured data.

The question as to whether to use random or chirp excitation is rather dependent upon a number of factors rather than purely the excitation signals themselves. If everything was equal, and absolute control of the gains was possible, then the approaches with the best crest factors i.e. the optimal sweep approach should be used. The use of the methods developed in this study should be employed on actual flight flutter tests to investigate their applicability in practice.

7.   Future Work

1. The excitation signals described above should be compared to more traditional approaches in real life flight flutter testing.   Some of the methods are to be implemented in the flight test of an F-18 aircraft at NASA Dryden sometime in the near future.

2. The consequences of the clipping methods giving near sine sweep type signals should be investigated further. Does this mean that the optimum broad band signal is a sine sweep ? or is this just a consequence of the algorithm used, and should some means of 'mixing' up the frequency content in the Gerchburg-Saxton algorithm be explored.

3. Comparison of the developed methods should be made with excitation signals based upon solely (+1, -1) or (+1,0,-1) elements. Such methods would give very good crest factors but would not necessarily give exactly the desired frequency content. The consequences of rate expectations of such signals should also be taken into account.

4. Consideration should be made of the use of force appropriation type methods for flight flutter testing. Such methods are successfully used in ground testing to separate modes with very close natural frequencies and significant modal interaction, and so the application to flight testing would seem to be a natural step.

8. References

1. R.L. Bisplinghoff, H Ashley & R.L. Halfman, Aeroelasticity', Dover 1996.

2. M.W. Kehoe, A Historical Overview of Flight Flutter Testing, AGARD SMP Meeting on Advances in Aeroservoelastic Testing and Data Analysis, AGARD Conference Proceedings 566, Paper 1, 1995.

3. J.E. Cooper, Parameter Estimation Methods for Flight Flutter Testing, AGARD SMP Meeting on Advances in Aeroservoelastic Testing and Data Analysis, AGARD Conference Proceedings 566, Paper 10, 1995.

4. J.E. Cooper & J.R. Wright, On the Optimisation of Random Signals with Minimum Rate for Flight Flutter Testing, Proceedings of the International Forum on Aeroelasticity and Structural Dynamics, pp299 – 306, 1997.

5. A.P. Burrows, J.R. Wright & J.A. Coote, Optimal Excitation for Aircraft Flutter Testing, IMechE Journal of Aerospace Engineering, 1995.

6. R.G. White, Spectrally shaped transient forcing functions for frequency response testing, Journal of Sound and Vibration, Vol 23(2), pp 307-318, 1972.

7. P. De Fonseca, J.E. Cooper & J. Swivers, Optimal Random Excitation, Proceedings of ISMA21, pp903 – 913, 1996.

8. J.S. Bendat & A.G. Piersol, Random Data: Analysis and Measurement Procedures, John Wiley & Sons, 1971.

9. Bendat & A.G. Piersol, Engineering Applications of Correlation and Spectral Analysis, John Wiley & Sons, 1980.

10. M.R. Schroeder 'Synthesis of Low-Peak Factor Signals and Binary Sequenceswith Low Autocorrelation' IEEE Trans IT v16 pp85-89. 1970.